Environmental Science & Technology

pubs.acs.org/est

Article

Long-Term Succession Shows Interspecies Competition of *Geobacter* in Exoelectrogenic Biofilms

Xuejun Yan,[#] Qing Du,[#] Quanhua Mu, Lili Tian, Yuxuan Wan, Chengmei Liao, Lean Zhou, Yuqing Yan, Nan Li, Bruce E. Logan, and Xin Wang*

Cite This: *Environ. Sci. Technol.* 2021, 55, 14928−14937

Read Online

ACCESS | Metrics & More | Article Recommendations | Supporting Information

ABSTRACT: *Geobacter* spp. are well-known exoelectrogenic microorganisms that often predominate acetate-fed biofilms in microbial fuel cells (MFCs) and other bioelectrochemical systems (BESs). By using an amplicon sequence variance analysis (at one nucleotide resolution), we observed a succession between two closely related species (98% similarity in 16S RNA), *Geobacter sulfurreducens* and *Geobacter anodireducens*, in the long-term studies (20 months) of MFC biofilms. *Geobacter* spp. predominated in the near-electrode portion of the biofilm, while the outer layer contained an abundance of aerobes, which may have helped to consume oxygen but reduced the relative abundance of *Geobacter*. Removal of the outer aerobes by norspermidine washing of biofilms revealed a transition from *G. sulfurreducens* to *G. anodireducens*. This succession was also found to occur rapidly in co-cultures in BES tests even in the absence of oxygen, suggesting that oxygen was not a critical factor. *G. sulfurreducens* likely dominated in early biofilms by its relatively larger cell size and production of extracellular polymeric substances (individual advantages), while *G. anodireducens* later predominated due to greater cell numbers (quantitative advantage). Our findings revealed the interspecies competition in the long-term evolution of *Geobacter* genus, providing microscopic insights into *Geobacter*'s niche and competitiveness in complex electroactive microbial consortia.

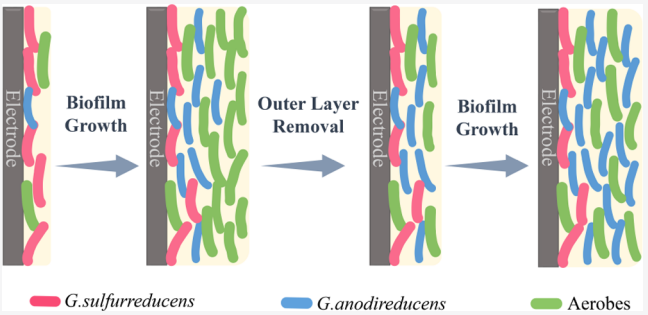

KEYWORDS: *bioelectrochemical systems, Geobacter sulfurreducens, Geobacter anodireducens, biofilm stratification, aerobes, outer biofilm removal, interspecies succession, growth advantage*

INTRODUCTION

Extracellular electron transfer (EET) enables some microorganisms to respire using metal oxides in minerals, promoting the biogeochemical cycle of chemical elements.[1−3] Based on this special respiration mode, exoelectrogenic biofilms, the core of microbial fuel cells (MFCs) and other bioelectrochemical systems (BESs), can be easily obtained by inserting biased electrodes into anaerobic natural microbial suspensions.[4] These devices can be further manipulated by controlling the electrode potentials to achieve functions such as bioelectricity generation, biohydrogen production, desalination, or production of value-added chemicals.[5−7] In these BESs, *Geobacter* spp. become predominant based on their efficient EET mediated by c-type cytochromes and production of electrically conductive nanowires.[8−10]

A total of 19 strains of *Geobacter* have been isolated from different environments, and all of them achieve optimal growth and EET efficiency under highly reducing conditions with acetate as the preferred substrate.[10] In the case of soil remediation or actual wastewater treatment, it is difficult to provide such an ideal microniche for *Geobacter* based on only acetate as a substrate and a complete lack of oxygen.[11] The presence of alternate electron acceptors and many different substrates enrich microorganisms with different metabolisms that include fermentative,[12] aerobic,[13,14] and nitrate respiration.[15] Due to the competitive pressure caused by these variable conditions, *Geobacter* spp. have ranged from 3 to 88% in abundance in exoelectrogenic biofilms, although they are usually the main contributor to EET.[12,16−18] *Geobacter* spp. have been found to inhabit the inner biofilms close to the electrode surface, while microorganisms with other metabolisms grow in the outer layers near the suspensions at variable conditions.[19−21]

Both environmental factors and bacterial autogenic characteristics determined by heredity will presumably result in the dominance of different *Geobacter* spp. in exoelectrogenic biofilms.[22−25] Specific *Geobacter* species have different

Received: May 9, 2021
Revised: August 16, 2021
Accepted: October 13, 2021
Published: October 22, 2021

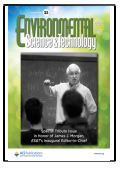

https://doi.org/10.1021/acs.est.1c03010
Environ. Sci. Technol. 2021, 55, 14928−14937

advantages in biofilm formation[26,27] as well as tolerance to environmental stresses including oxygen,[26,28] electric field strength,[24] and medium salinity.[29] These differences provide possibilities to drive the predominance of different species of *Geobacter* in biofilms. For example, based on the phylogenetic affiliation, three core OTU clusters affiliated with different *Geobacter* species were found to have specific responses to oxygen variables caused by changes in electrode spacing in air-cathode MFCs.[22] However, it is difficult for conventional analysis methods to distinguish some closely related species, such as *Geobacter sulfurreducens* and *Geobacter anodireducens* (98% similarity in 16S rRNA),[30] both of which are common in BESs.[18,23,24,31] Therefore, the evolution of *Geobacter* species composition in biofilms may not have been sufficiently examined over long periods of time.

The objective of this study was to explore the interspecific relationship of *Geobacter* spp. that develop over time in the long-term (20 months) operation of MFC biofilms. To achieve this goal, an exact amplicon sequence variant (ASV) analysis (at one nucleotide resolution) was used to distinguish the relative predominance of even very closely related *Geobacter* spp.[24,32] Through microbial community analysis and electroactivity detection of the outer biofilms, we monitored the evolution of *Geobacter* in MFC biofilms over time and space. To reduce the influence of aerobes on *Geobacter* spp., a part of the outer biofilm mainly composed of aerobes was removed, for the biofilms to re-evolve. To better understand the competition between the two *Geobacter* species that evolved in the MFC biofilm over time, we conducted co-culture tests in oxygen-free BESs to examine the changes in the predominance of these two microorganisms over time.

MATERIALS AND METHODS

Reactor Configuration. Experiments were conducted using either air-cathode MFCs inoculated with wastewater or oxygen-free BESs inoculated with pure cultures. The air-cathode MFCs (duplicates) were single-chamber reactors (4 cm in length with an inner plexiglass cylindrical chamber of 7 cm in diameter and volume of 154 mL). The anodes, that is, three carbon fiber brushes (3 cm in diameter and 3 cm in length) with a titanium core were inserted into the prefabricated holes with triangular distribution in the plexiglass partition. Activated carbon air-cathodes (38 cm^2) were fabricated by a rolling-press procedure, as previously described.[33] Customized large BESs (L-BESs, 100 mL in volume) were used in some tests to detect the electroactivity of MFC planktonic cells removed from the biofilms. These BESs contained a graphite rod working electrode, a plain platinum sheet counter electrode, and an Ag/AgCl reference electrode, as previously described.[34]

Single-chambered, three-electrode BESs (15 mL in volume) constructed with serum bottles were used to examine the competition of two *Geobacter* spp. under oxygen-free conditions. A graphite sheet (1 × 1.5 × 0.3 cm) was used as the working electrode, and the counter electrode was stainless steel mesh (1 × 1.5 cm, Type 304N, 60 meshes). All potentials obtained and reported here were relative to Ag/AgCl reference electrodes (4 M KCl, 0.197 V vs standard hydrogen electrode). Pretreatment and installation of electrodes were carried out as previously described.[35]

Long-term Operation of MFCs. MFCs were inoculated with domestic wastewater collected from the wastewater treatment plant in the Jinnan campus of Nankai University. The medium used for MFC tests was 1 g/L sodium acetate in a 50 mM phosphate buffer solution (PBS: Na_2HPO_4, 4.58 g/L; NaH_2PO_4, 2.13 g/L; NH_4Cl, 0.31 g/L; KCl, 0.13 g/L; trace minerals, 12.5 mL/L; vitamin solution, 5 mL/L).[34] The medium was refreshed when the cell voltage decreased to <20 mV, forming a cycle that typically had a duration of 2 days.[17] The external resistance was 1000 Ω during the initial stage of biofilm acclimation and then it was reduced to 100 Ω when reproducible maximum voltages were obtained in two consecutive cycles. All reactors were operated at 25 ± 2 °C for 20 months. Cathodes were replaced every month with a new one to avoid a substantial decrease in performance over time.[33,36] Electrochemical as well as chemical tests, including cyclic voltammetry (CV), maximum power densities, open-circuit potentials (OCP), chemical oxygen demand (COD), pH, and dissolved oxygen (DO), were conducted every month (see detailed methods in the Supporting Information).

Co-cultures of *Geobacter* Strains in BESs. Co-cultures of *G. sulfurreducens* and *G. anodireducens* were examined in oxygen-free BESs along with tests using single pure cultures as controls. *G. sulfurreducens* PCA (ATCC-51573)[37] was resuscitated from laboratory frozen stocks, and *G. anodireducens* SD-1 was provided by Sun.[30] PCA was cultured in NBAF medium containing 15 mM sodium acetate and 40 mM fumaric acid.[38] SD-1 was grown in a modified acetate-ferric citrate (FcA) medium consisting of 30 mM carbonate buffer solution (CBS: $NaHCO_3$, 2.5 g/L; NH_4Cl, 1.5 g/L; NaH_2PO_4, 0.6 g/L; KCl, 0.1 g/L; mineral solution, 10 mL/L; vitamin solution, 10 mL/L), 20 mM sodium acetate, and 40 mM ferric citrate.[37] To completely exclude the influence of other electron acceptors (iron and fumaric acid) in the growth media, both strains were initially grown on graphite electrodes in BESs (bias voltage of 0.7 V) to harvest abundant clean cells,[29,35,39] and these cells were then used as the inocula for co-culture tests.

The collected cells were resuspended in sterile medium and then repeatedly pipetted to disperse the cells producing the final inoculum with an optical density at 600 nm (OD_{600}) of 0.1. The sample was split into three experimental groups: only PCA (marked as group PCA), only SD-1 (marked as group SD-1), and an equal mixture of both strains (marked as group co-culture). All operations followed anaerobic and aseptic procedures (see details in the Supporting Information) before connecting the reactors to a multichannel potentiostat (CHI 1000C, CH Instrument, Shanghai, China) with a potential of 0 V. The medium, containing 1 g/L sodium acetate and 30 mM CBS, was refreshed when the current was below 0.2 mA, starting a new cycle. All BESs were cultivated at 30 °C for five cycles.

Electroactivity Detection and Removal of Outer Layers of MFC Biofilms. To examine the extent to which outer biofilms contained exoelectrogens, the planktonic cells that could be dislodged from the outer layer by slight shaking were collected as inocula to grow new biofilms in sterile L-BESs every month. The suspension solution at the end of each cycle was supplemented with 50 mM PBS (1:1, v/v), as well as 1 g/L sodium acetate, and then flushed with a N_2/CO_2 (80/20, v/v) gas mixture for 30 min to remove DO. Currents were monitored every 100 s using chronoamperometry by a multichannel potentiostat (0 V vs Ag/AgCl).

After 11 months, the outer biofilm was removed by disrupting cohesion through direct contact with norspermidine (NP, M033008, MREDA, USA) in the medium. NP can

https://doi.org/10.1021/acs.est.1c03010
Environ. Sci. Technol. 2021, 55, 14928−14937

dissolve extracellular polysaccharides and DNA that contribute to biofilm adhesion.[40,41] The optimal concentration of NP, which can remove the outer layer lacking *Geobacter* but preserve the inner *Geobacter* to the greatest extent, was determined to be 7 mM by pre-experiments (see the Supporting Informaion for details). The medium containing 7 mM NP was added to the MFC, then mixed by lightly shaking the reactor, and then left on the benchtop. After 12 h of this static exposure, the MFC medium was next replaced with a fresh NP-free electrolyte, and the exfoliated biofilm was removed. Following three normal cycles with NP-free solutions, there was no additional biofilm in the suspension, indicating that the outer layers of the biofilm had been removed. The tolerance test of two *Geobacter* strains to NP was conducted in modified FcA media (see the Supporting Information for details).

Microbial Community Analysis. While testing the electroactivity of the outer biofilm every month, planktonic cell samples were collected by centrifugation (13,700*g*, 10 min). Simultaneously, MFC biofilms were also sampled by cutting carbon fibers with sterile scissors. Genomic DNA was extracted using the Soil Genomic DNA Kit (CW2091S, Com Win Biotech Co., Ltd., China), following the procedures of the manufacturer. The hypervariable V4 region of 16S rRNA was amplified by PCR with the universal primer set of 515F (5′-GTGCCAGCMGCCGCGGTAA-3′) and 806R (5′-GGACTACHVGGGTWTCTAAT-3′). All amplicons were subsequently sequenced by Illumina MiSeq sequencing platform in Novogene (Beijing, China).

The demultiplexed Illumina-sequenced dataset without barcode or adapters was processed by the open-source R package DADA2,[42] including filtering, trimming, amplicon error correction, ASV abundance estimation, and chimera removal. Each ASV was trimmed to 253 ± 3 nucleotides in length based on the quality score visualization. The resulting ASV table was a higher resolution analogue of the OTU table, which tallied the number of times each exact ASV was observed in each sample. Taxonomic assignment was performed against the Ribosomal Database Project (RDP) 16 database using the implementation of the naive Bayesian classifier method. The abundance of aerobic and anaerobic microorganisms was predicted based on sequencing data with the help of the BugBase algorithm tool (https://bugbase.cs.umn.edu).[43] The visualization of the results was realized by R language. All raw sequence data were uploaded to the NCBI Sequence Read Archive (SRA) with accession number PRJNA693176.

Growth Status Detection of *Geobacter* Strains. *Geobacter* biofilms cultured for different times in co-culture tests were completely scraped off by sterile knives and collected in aseptic centrifuge tubes. These samples were resuspended in PBS (50 mM) sterilized by 0.22 μm filters to obtain biofilm suspensions for subsequent biomass analysis. To obtain a total protein extract, the biofilm suspension was centrifuged (13,700*g*, 10 min); then, 0.3 M NaOH was added, and the centrifugation tube was placed in a water bath at 37 °C for 30 min.[33] A modified cation exchange resin method was used to extract extracellular polymeric substances (EPS) from the biofilm suspension in cycle 5 (see the Supporting Information for details).[44] The bicinchoninic acid method was applied to determine the protein content, following the instructions of the protein quantification kit (E112-02, Vazyme, Nanjing, China).[16] The polysaccharide content was measured by the phenol−sulfuric acid method.[45] The biofilm suspension was negatively stained with 2% uranyl acetate on a carbon-coated copper grid and then examined with a transmission electron microscope (TEM) (HT7700, Hitachi, Japan) operating at 80 kV to observe the cell size.

Cell numbers in pure *Geobacter* biofilms were quantified by combining quantitative PCR (qPCR) with cell counting.[25] Two PCR primers were specially designed for the two strains with DNAMAN software tool (Table S1). Their expected amplification products were also verified by 1.5% agarose gel electrophoresis (Figure S2) and sequencing analysis. Genomic DNA was extracted from the biofilm suspension using the Soil Genomic DNA Kit. All qPCR tests were conducted in an authorized real-time PCR system (IQ5, Bio-Rad, CA, USA). Standard curves were constructed based on the threshold cycle (CT) values for a 10-fold dilution series of DNA extracted from pure culture. To obtain the initial concentrations of standard DNA, cells were counted through a cell counting box combined with confocal laser scanning microscopy (LSM880, Zeiss, Oberkochen, Germany). The qPCR reaction system and amplification program can be found in the Supporting Information. For each qPCR run, melting curves and negative controls (DNase-free water) were simultaneously conducted. At least three independent biological replicates and three technical replicates were used for all experiments.

RESULTS

Performance of MFC Biofilms in Long-term Growth. Cell voltages as well as OCP of both the anode and cathode were monitored over 14 months, showing relatively stable values (Figure 1A). By replacing the air-cathode monthly, cathodic performance decay resulting from salt precipitation and biofouling was minimized,[33,36] as shown by a consistent cathode OCP of 76 ± 14 mV. The anode required 3 months to

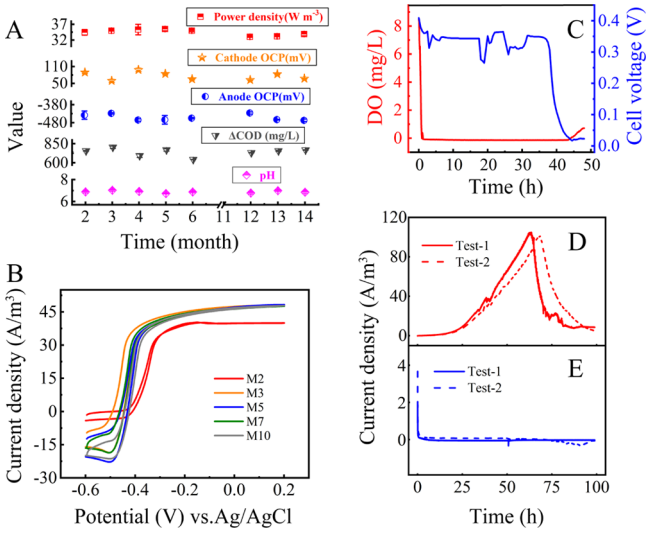

Figure 1. Performance of MFC in 14 months. (A) Maximum power density, OCP of anode and cathode, change of COD in one cycle (ΔCOD), and pH of the electrolyte monitored over 14 months. (B) Turnover CVs of anodic biofilms from month 2 (M2) to month 10 (M10). (C) Representative changes in cell voltage and DO during one cycle under an external resistance of 100 Ω. Representative time−current curves of L-BESs inoculated by planktonic cells in MFCs collected (D) in the initial 4 months and (E) from month 5 to 11. Test-1 and Test-2 are two parallel experimental groups.

https://doi.org/10.1021/acs.est.1c03010
Environ. Sci. Technol. 2021, 55, 14928−14937

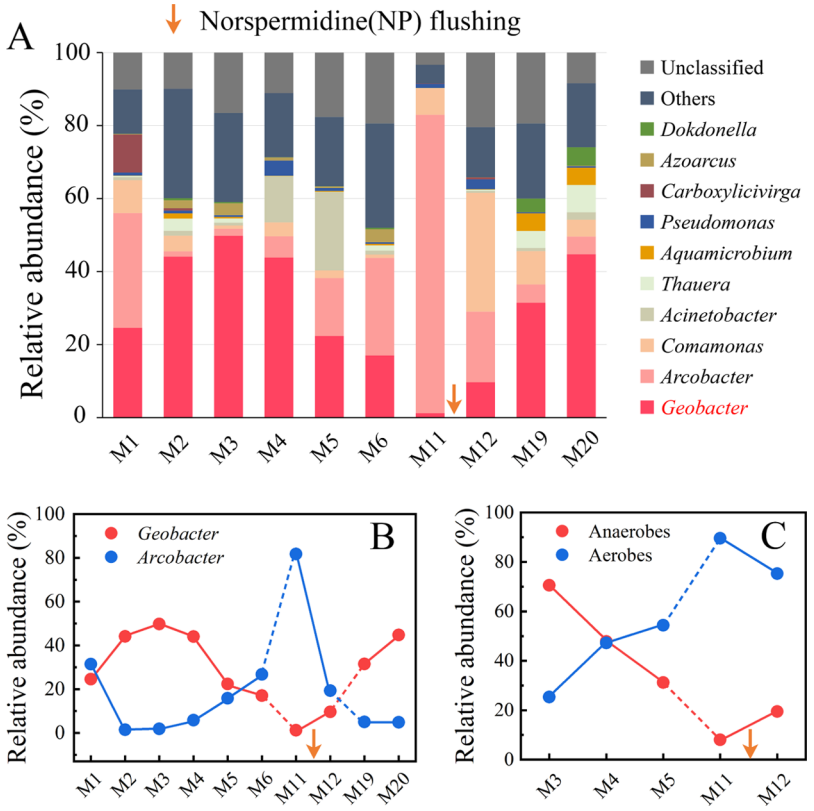

Figure 2. Succession of microbial communities of MFC biofilms over 20 months. (A) Taxonomic classification of bacterial communities at the genus level (top 10). The relative abundance variation trend of (B) *Geobacter* and aerobic *Arcobacter*, (C) anaerobes and aerobes. M1−M20 indicate results from months 1 to 20. The values between two adjacent months are connected by solid lines, while the changes between nonconsecutive months are represented by dotted lines. The orange arrow indicates the removal of a part of the outer biofilm with 7 mM NP.

reach a stable maximum current of 48 ± 0.3 A/m^3 in CV tests (Figure 1B). The anode OCP was steady over the next 11 months (until month 14) at −457 ± 16 mV (Figure 1A). The MFCs had a stabile maximum power density based on the polarization data of 34 ± 0.9 W/m^3, with a COD removal of 740 ± 51 mg/L (90 ± 3.0%), and a final pH of 6.9 ± 0.1.

DO was present in the medium, and oxygen can also leak into the electrolyte through the porous cathode.[13] The medium added to the MFC initially contained DO of 8.5 mg/L, which was rapidly depleted to ∼0 mg/L after 1.2 h (Figure 2C), consistent with its rapid removal noted in previous studies.[14,16] At the end of each cycle, most of the substrate was depleted, which was reflected by the drop in the voltage value, and the DO slightly increased in solution to a concentration of ∼0.7 mg/L.

The electroactivity of the outer layer of the biofilms appeared to change over time, as demonstrated through the changes in the starting current of L-BESs inoculated by planktonic cells collected over time (Figure 1D,E). In the initial 4 months, exoelectrogens were present in the planktonic cells, as demonstrated by a rapid colonization on graphite rods when the solution was transferred to new devices (L-BESs) (Figure 1D). The maximum current density with these transferred solutions averaged 103 ± 2 A/m^3 after 65 h. However, transfers of the solutions from the MFC in subsequent months (5−11) failed to produce current in L-BESs (Figure 1E). This loss of electroactivity suggested a relative absence of exoelectrogens in the outer layers as the biofilm thickened (Figure S3A,B).

Abundance and Distribution of *Geobacter* in Long-term Growing Biofilms. Like most biofilms in BES-fed acetate,[46,47] *Geobacter* was found to be the dominant exoelectrogenic genus in our systems. Although its abundance in month 1 (25%) was lower than that of aerobic *Arcobacter* (31%),[48] *Geobacter* exhibited an upward trend in the next 2 months (2−3), as shown by an average value of 47 ± 4.0%, which was much higher than that of *Arocobacter* (1.7 ± 0.33%), *Comamonas* (2.6 ± 2.4%), and other genera (Figure 2A). The increasing proportion of *Geobacter* in the biofilms also corresponded to an increase of the maximum current densities obtained in CV tests (Figure 1B). In month 2−3, *Geobacter* were 7.0% of the planktonic communities and enriched to 73% of the genera identified in the biofilms of transferred reactors (L-BES biofilm), dominating rapid subcultivation in L-BES reactors (Figure S4).

After increasing in numbers for 3 months, the abundance of *Geobacter* began to decline over time, with an increase of the aerobic microorganism with *Arcobacter* as the representative genus in the biofilms from cutting and sampling fibers (Figure 2B,C). Aerobes accounted for 54% of the identified genera in month 5 and began to surpass anaerobes (31%). By month 11, there was only 1.2% of *Geobacter* in the biofilm, much less than *Arcobacter* (82%). Although the biofilm was constantly evolving, the stable maximum current density was observed in CVs from month 3 (Figure 1B). The first-order derivative of CV current also showed the same symmetric main peak that appeared at −0.42 ± 0.02 V (Figure S5), which was close to the midpoint potentials of the outer membrane cytochromes secreted by *Geobacter*,[49] implying that the dominant EET

https://doi.org/10.1021/acs.est.1c03010
Environ. Sci. Technol. 2021, 55, 14928−14937

genera was always *Geobacter*. While the outer biofilm lacked sufficient *Geobacter* to produce rapid current generation in L-BESs in month 5, *Geobacter* still accounted for 22% of the whole biofilm, similar to that in month 1 (25%) (Figure 2A). These results showing *Geobacter* consistently present in the biofilm but not the suspension solution indicated an uneven distribution of *Geobacter* in the biofilm and suggested an increase of other types of microorganisms in the outer biofilm over time rather than an absolute decrease in the numbers of total *Geobacter*.[16] Therefore, it was concluded that *Geobacter* mainly existed in the near-electrode inner layer to achieve efficient EET,[20] while the outer layer was dominated by aerobes using oxygen in the fresh medium and leaking through the cathode.

The ASV analysis at the species level revealed that *Geobacter* spp. in MFC biofilms were mainly composed of *G. sulfurreducens* and *G. anodireducens* and that these two species showed a dynamic evolution over time (Figure 3). In the first 5

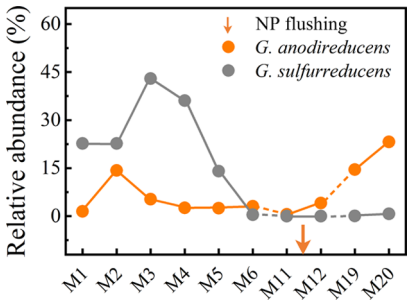

Figure 3. Relative abundance variation trend of *G. sulfurreducens* and *G. anodireducens* in MFC biofilms based on ASV analysis. M1−M20 indicate results from months 1 to 20. The values between two adjacent months are connected by solid lines, while the changes between nonconsecutive months are represented by dotted lines. The orange arrow indicates the removal of a part of the outer biofilm with 7 mM NP.

months, *G. sulfurreducens* accounted for 75 ± 17% of *Geobacter* genus and generally followed a trend consistent with total *Geobacter* in the biofilm (Figures 2B and 3). The abundance of *G. sulfurreducens* in the total species identified in the biofilm reached the peak (43%) in month 3 but declined rapidly in subsequent months (4−6) due to the increase in the total number of bacteria, especially aerobes (Figures 2B and 3). *G. anodireducens* was also found in month 4−6, with a relatively stable content of 2.8 ± 0.33% in the total species of biofilms, but this proportion also dropped to only 0.57% in month 11.

Removal of Outer Biofilms Increased the Relative Abundance of *Geobacter* spp. To reduce the influence of aerobes on the relative content of *Geobacter* spp., a part of the outer biofilm was removed using NP (7 mM) treatment at the end of month 11 (Figure S3B,C). After that, the OCP of the anode remained stable (Figure 1A), but the biofilm composition changed. The dominant *Arcobacter* abundance decreased from 82% in month 11 to 19% in month 12, although the overall percentage of aerobes decreased by only 14% due to the increase of other genera, especially *Comamonas* (Figure 2).[50,51] *Geobacter* occupied 9.7% of biofilms in month 12, nearly 8 times higher than that in month 11. The abundance of *Geobacter* also increased in the planktonic community (Figure S4), and thus the subcultivation of planktonic cells in new reactors (L-BES) again showed rapid current generation (Figure S6). These results indicated that the NP treatment achieved the expected goal of increasing the relative abundance of *Geobacter* by stripping off the outer biofilm that contained primarily aerobes.

The content of *Geobacter* in the biofilms progressively increased in the subsequent months (12−20), reaching 45% in month 20, which was close to the peak in month 3 (50%) (Figure 2B). However, the dominant species was transformed to *G. anodireducens* with an abundance of 47 ± 5% of all *Geobacter* in this period, while *G. sulfurreducens* was nearly undetectable (Figures 2B and 3). This succession of the two *Geobacter* spp. was not a result of NP's specific selectivity because their tolerance to NP was equivalent (Figure S7). Also, the relative predominance of these two species had already reversed in month 6, as the percentage of *G. anodireducens* (3.1%) surpassed *G. sulfurreducens* (0.43%) (Figure 3). By month 11, *G. anodireducens* was 46% of the total *Geobacter*, although *G. anodireducens* only accounted for 0.57% of the entire biofilm with an overall low abundance of *Geobacter* of 1.2% (Figures 2B and 3). With the increase in *Geobacter* abundance resulting from the removal of the outer layer, the percentage of *G. anodireducens* increased to 4.1% in month 12, furthering the transition from *G. sulfurreducens* to *G. anodireducens*.

Growth of *G. sulfurreducens* and *G. anodireducens* as Pure Cultures. To further examine the factors that impact competition between *G. sulfurreducens* PCA and *G. anodireducens* SD-1, pure culture experiments were carried out in oxygen-free reactors (L-BESs) to explore their growth on the electrode applied with a potential set at 0 V (vs Ag/AgCl). In the first cycle, the similar maximum current density growth rate (0.12 ± 0.02 A/m^2/h) was achieved significantly ($p < 0.001$, $n = 3$) faster for strain PCA (37.2 ± 0.7 h) compared to SD-1 (64.0 ± 3.2 h), but the maximum current densities were similar (~3 A/m^2) (Figures S8 and 4A). After this first cycle, the greater highest current densities in every cycle were always obtained by strain SD-1, which was likely due to a significantly ($p < 0.05$, $n = 3$) higher protein content of SD-1 on the electrode (Figure 4B,C). Many studies have shown that current initially had a positive linear correlation with protein biomass but then eventually reached a stable plateau due to the limitations of pH gradients and metabolic heterogeneity in thick biofilms.[39,52] With a high protein biomass, SD-1 began to obtain a reproducible highest current density of 5.2 ± 0.2 A/m^2 from cycle 3, while PCA was still in its rising stage of current generation until cycle 5 (Figure 4B).

SD-1 was always present in significantly ($p < 0.01$, $n = 3$) greater cell numbers than PCA (Figure 4D). Normalizing the protein content by cell numbers in each cycle, PCA (8.77 ± 1.96 × 10^{-7} μg per cell) was 2.6 times more abundant than SD-1 (3.41 ± 0.31 × 10^{-7} μg per cell) based on single cell protein yields (Figure 4C,D). However, the number of PCA cells (0.85 ± 0.20 × 10^{12} cells/m^2) was only ~1/3 of SD-1 (2.59 ± 0.40 × 10^{12} cells/m^2) in the first cycle, so that the total protein content had comparable values (PCA, 0.90 ± 0.04 g/m^2 and SD-1, 0.95 ± 0.16 g/m^2) and thus produced similar high current densities (3.0 ± 0.2 A/m^2) (Figure 4B−D). After that, SD-1 cell numbers increased at an average rate of 3.11 × 10^{12} cells/m^2 per cycle, which was 3.2 times larger than PCA (0.98 × 10^{12} cells/m^2 per cycle), higher than their ratio of protein biomass of a single cell (2.6) (Figure S9). This difference led to the SD-1 biomass based on protein to increase at the rate of 1.5 times (0.88 g/m^2) over PCA (0.60 g/m^2)

https://doi.org/10.1021/acs.est.1c03010
Environ. Sci. Technol. 2021, 55, 14928−14937

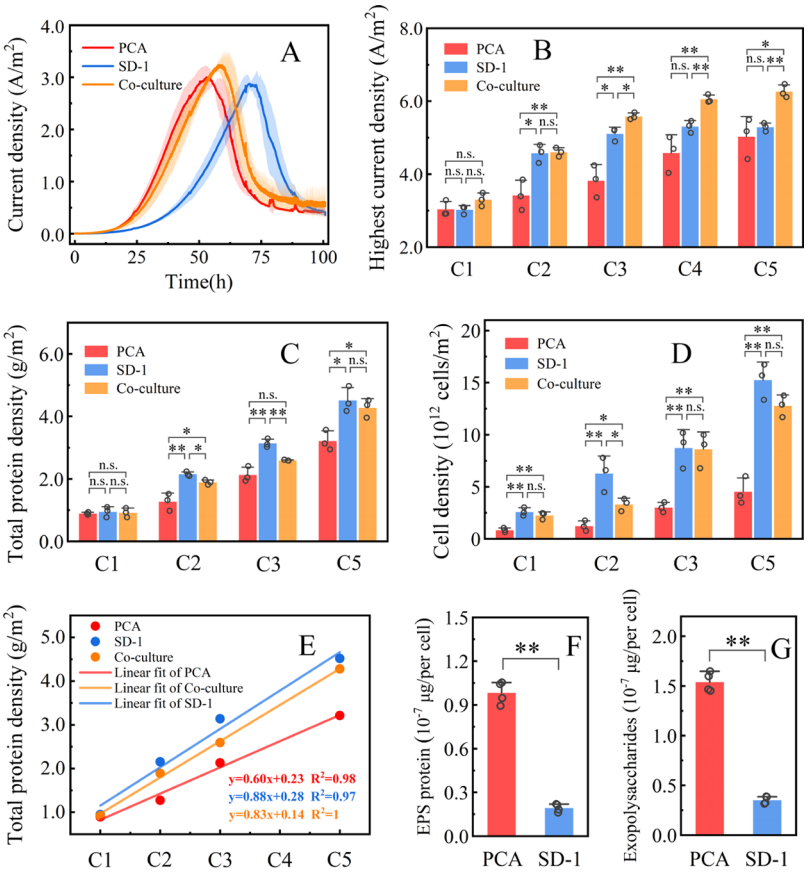

Figure 4. Performance and growth status of biofilms formed by *G. sulfurreducens* PCA and *G. anodireducens* SD-1 in pure culture or co-culture. (A) Time−current curves in the first cycle. (B) Maximum current density, (C) total protein density, (D) growth rate of total protein, and (E) cell number density quantified using qPCR in cycles 1−5. (F) Extracellular protein and (G) exopolysaccharides in extracted EPS were averaged per cell. All biofilms were cultured at a potential of 0 V (vs Ag/AgCl). C1−C5 represented the results at the end of cycles 1−5. Data presented are the mean ± SD (n = 3 or 4), and error bars represent standard deviations. Statistical significance ($^{n.s.}p > 0.05$, $^{*}p < 0.05$, $^{**}p < 0.01$) was assayed using unpaired t test via SPSS 26.

(Figure 4E). Taken together, SD-1 relied on the advantage of cell numbers to produce more biomass and higher current.

Although both strains were short rods, their cell sizes were different (Figure S10), consistent with previous reports.[30,37] Calculating cell volumes based on cylinders, PCA (0.17 μm^3, 1.37 μm length, 0.39 μm diameter, n = 13) was 1.8 times larger than SD-1 (0.09 μm^3, 1.62 μm length, 0.27 μm diameter, n = 14). The larger cell size of PCA, therefore, contributed more intracellular protein, and the extracellular protein per cell (0.98 ± 0.08 × 10^{-7} μg) was also significantly ($p < 0.01$, n = 4) higher than that of SD-1 (0.19 ± 0.03 × 10^{-7} μg, Figure 4F). Furthermore, exopolysaccharide produced by a single cell of PCA (1.54 ± 0.10 × 10^{-7} μg) was 4.4 times higher than that by SD-1 (0.35 ± 0.04 × 10^{-7} μg), which could enhance cell adhesion at the early stage of biofilm formation (Figure 4G).[53]

Competition between *G. sulfurreducens* and *G. anodireducens* in Co-cultures. The competition between PCA and SD-1 was examined using co-cultures based on their relative abundances (Figure 5A). Due to the difference in the cell size, cell numbers at the same OD_{600} were not consistent,[25] and thus PCA was inoculated on the basis of cell numbers at a lower percentage (39 ± 5%) than SD-1. Nevertheless, the co-culture biofilm still showed a starting current curve very close to that of the group PCA (Figure 4A), suggesting that PCA was a more effective contributor in early biofilm formation. This speculation was further supported by the abundance change of PCA in cycle 1, as shown by an average increase by 10% to 49 ± 7% (Figure 5A). In the subsequent two cycles, SD-1 showed the same quantitative advantages in cell number as seen in the pure culture results (Figure 5B). At the end of cycle 3, the cell number of SD-1 was already 6.3 times that of cycle 1, while the factor for PCA was only 1.3. Therefore, the proportion of SD-1 reached 83 ± 4%, which was constant until cycle 5 (Figure 5A).

DISCUSSION

The genera *Geobacter* is known to dominate acetate-fed biofilms in BESs, but the results of our studies showed that there can be competition between strains, which may not have been previously evident based on the commonly used qPCR techniques due to their 98% similarity in 16S rRNA.[30] However, *G. sulfurreducens* is usually found to predominate among even different *Geobacter* species in exoelectrogenic biofilms.[18,25,31] *G. anodireducens* has also been found to be abundant in fed-batch laboratory BESs when care is taken to differentiate these two species.[23,24] Here, with the help of exact ASV analysis, the succession from *G. sulfurreducens* to *G. anodireducens* was observed in long-term cultured biofilms. The co-culture tests conducted in oxygen-free BES systems produced similar results to trends with naturally formed MFC biofilms (Figures 3 and 5A), indicating that *G. anodireducens* will become more predominant than *G.*

https://doi.org/10.1021/acs.est.1c03010
Environ. Sci. Technol. 2021, 55, 14928−14937

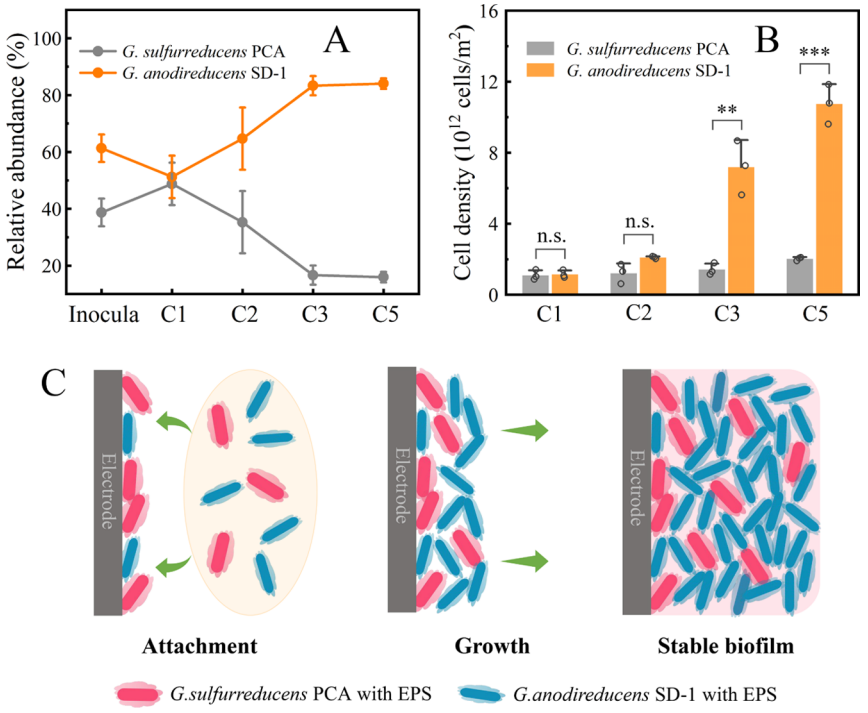

Figure 5. Competitive process of *G. sulfurreducens* PCA and *G. anodireducens* SD-1 in co-cultures. (A) Change in the relative abundance and (B) cell numbers of *G. sulfurreducens* PCA and *G. anodireducens* SD-1 in co-culture biofilms from cycle 1 (C1) to cycle 5 (C5). (C) Competitive model of *G. sulfurreducens* PCA and *G. anodireducens* SD-1. The green arrow indicates the direction of bacterial attachment or biofilm growth. Data presented are the mean ± SD ($n = 3$), and error bars represent standard deviations. Statistical significance ($^{n.s.}p > 0.05$, $^{*}p < 0.05$, $^{**}p < 0.01$, $^{***}p < 0.001$) was assayed using unpaired t test via SPSS 26.

sulfurreducens over time. This general finding suggests that intermittent oxygen exposure was not a critical cause of interspecific succession, as the transition from *G. sulfurreducens* to *G. anodireducens* was already underway before the outer biofilm containing predominantly aerobes was removed.

Pure and co-cultures of these two microorganisms in the BESs demonstrated more clearly, and over a shorter period, the relative attributes of *G. sulfurreducens* and *G. anodireducens* in the biofilm formation and development over time. When these two species coexist, a competitive model resulting from the difference in growth strategies can be proposed (Figure 5C). *G. sulfurreducens* tends to grow larger cells and secrete more EPS to quickly attach electrodes from the suspension (individual advantage) and thus to dominate early biofilms. However, the production of EPS may have a growth cost, inhibiting the rate of cell proliferation.[54] In contrast, the smaller *G. anodireducens* with less EPS has a greater rate of growth based on cell number. This growth mechanism gives *G. anodireducens* a quantitative advantage similar to that of a demographic dividend, eventually occupying the predominant niche in the stable biofilms. Indeed, *G. sulfurreducens* and *G. anodireducens* constructed a near-steady-state microflora with a ratio of 17:83 (~1:5) after cycle 3 (Figure 5A). The minor member *G. sulfurreducens* may not only provide scaffold-like structural support but also may accelerate the EET of *G. anodireducens* by secreting shared extracellular redox substances.[11,25,53] This steady-state structure of the co-cultured biofilm may be the optimal situation for the interactions between *G. sulfurreducens* and *G. anodireducens*, resulting in a significantly ($p < 0.05$) higher current density than either of the pure strains alone (Figure 4B). In addition to the cooperation in EET, these two *Geobacter* species could also use their respective growth advantages to complement each other, thereby maintaining the long-term functional stability of the biofilm. For example, when the relative abundance of *G. sulfurreducens* with individual advantages decreased due to the expansion of aerobes, *G. anodireducens* with the same efficient EET ability may rely on quantitative advantages to ensure the dominant niche of *Geobacter*. In the face of the competitive pressures caused by variable conditions, the cooperation among these functionally redundant exoelectrogens with different advantages may be a feasible strategy to realize the functional stability of BESs.[55]

The MFC biofilms, compared to the co-culture biofilms, needed much longer times for a succession to occur from *G. sulfurreducens* to *G. anodireducens*. The growth of these two species in MFC biofilms can be limited by their low content in the inoculum (wastewater)[56] and the insufficient electric field caused by the relatively low current density in MFCs.[24] Aerobes grown under intermittent oxygen may also compete for the substrate with both *Geobacter* species.[13] As the theoretical energy gain from the anaerobic respiration is lower than aerobic growth,[57] aerobic microorganisms usually have much higher cell yields than anaerobes,[58] which enable them to develop thicker biofilms than anaerobes. For example, *Pseudomonas denitrzpcans* could convert 45% of glutamate carbon into biomass when grown with oxygen, while the acetate assimilation rate of *G. sulfurreducens* was only 3.6−20% in the process of reducing iron.[58−60] Thus, these fast-growing outer aerobes resulted in a rapid decline in the relative abundance of *Geobacter* dominated by *G. sulfurreducens* (Figures 2A and 3). In this period, as a minority member of *Geobacter*, the growth advantage of *G. anodireducens* was not fully reflected because of the lack of sufficient cell base

https://doi.org/10.1021/acs.est.1c03010
Environ. Sci. Technol. 2021, 55, 14928−14937

compared to aerobes, and thus its succession relative to that of *G. sulfurreducens* progressed slowly in the inner biofilm. When the outer aerobes were partly removed by NP, *G. anodireducens*, which can better succeed by virtue of its quantitative advantage in biofilm mass, also increased the competitiveness of the entire *Geobacter* genus in long-term operation. From the engineering perspective, the periodic removal of the outer fouling-like layer of biofilms is helpful to keep *Geobacter* dominant in the microbial community and has the additional benefit to select another highly electroactive strain *G. anodireducens* by providing a larger ecological space for the interspecific competition.

Geobacter are increasingly recognized important in the biogeochemical cycling of metals (especially iron and manganese) coupled with nutrient elements.[61] With the help of a well-developed exoelectrogenic and conductive network, different *Geobacter* spp. can build a syntrophic relationship to achieve efficient cell-to-cell electron exchange.[62,63] Also, the ecological value of interspecific competition revealed herein may be to form an efficient and competitive *Geobacter* species group to survive in the complex microbial consortia. The transition from *G. sulfurreducens* to *G. anodireducens* in exoelectrogenic biofilms for 20 months highlighted the importance of the interspecific competition of *Geobacter*, which showed the necessity of exploring microbial interactions related to *Geobacter* at the species level in a complex electroactive microbial community. Furthermore, it may be a feasible strategy to make full use of the competitive advantages of different species to improve the competitiveness of *Geobacter* in anaerobic underground environments.

■ ASSOCIATED CONTENT

Supporting Information

The Supporting Information is available free of charge at https://pubs.acs.org/doi/10.1021/acs.est.1c03010.

Electrochemical and chemical analyses; anaerobic and aseptic procedures; selection of the optimal NP concentration; tolerance tests of *Geobacter* to NP; EPS extraction; qPCR settings; primer sequences; effect of NP concentrations on biofilms; image of agarose gel electrophoresis; images of MFC biofilms; communities of MFC planktonic cells; first-order derivative on CVs of MFC biofilms; time−current curves of L-BESs after NP treatment; effect of NP on two *Geobacter* strains; current density growth rate of pure culture biofilms in cycle 1; cell density growth rate in co-culture test; and transmission electron micrographs of two *Geobacter* strains (PDF)

■ AUTHOR INFORMATION

Corresponding Author

Xin Wang − *MOE Key Laboratory of Pollution Processes and Environmental Criteria/Tianjin Key Laboratory of Environmental Remediation and Pollution Control, College of Environmental Science and Engineering, Nankai University, Tianjin 300350, China;* orcid.org/0000-0002-3522-5627; Phone: (86)18722292585; Email: xinwang1@nankai.edu.cn; Fax: (86)22-23501117

Authors

Xuejun Yan − *MOE Key Laboratory of Pollution Processes and Environmental Criteria/Tianjin Key Laboratory of Environmental Remediation and Pollution Control, College of Environmental Science and Engineering, Nankai University, Tianjin 300350, China*

Qing Du − *MOE Key Laboratory of Pollution Processes and Environmental Criteria/Tianjin Key Laboratory of Environmental Remediation and Pollution Control, College of Environmental Science and Engineering, Nankai University, Tianjin 300350, China*

Quanhua Mu − *Department of Chemical and Biological Engineering, Hong Kong University of Science and Technology, Hong Kong, China*

Lili Tian − *MOE Key Laboratory of Pollution Processes and Environmental Criteria/Tianjin Key Laboratory of Environmental Remediation and Pollution Control, College of Environmental Science and Engineering, Nankai University, Tianjin 300350, China*

Yuxuan Wan − *MOE Key Laboratory of Pollution Processes and Environmental Criteria/Tianjin Key Laboratory of Environmental Remediation and Pollution Control, College of Environmental Science and Engineering, Nankai University, Tianjin 300350, China*

Chengmei Liao − *MOE Key Laboratory of Pollution Processes and Environmental Criteria/Tianjin Key Laboratory of Environmental Remediation and Pollution Control, College of Environmental Science and Engineering, Nankai University, Tianjin 300350, China*

Lean Zhou − *School of Hydraulic Engineering, Changsha University of Science & Technology, Changsha 410114, China*

Yuqing Yan − *MOE Key Laboratory of Pollution Processes and Environmental Criteria/Tianjin Key Laboratory of Environmental Remediation and Pollution Control, College of Environmental Science and Engineering, Nankai University, Tianjin 300350, China*

Nan Li − *School of Environmental Science and Engineering, Tianjin University, Tianjin 300072, China;* orcid.org/0000-0002-5852-2325

Bruce E. Logan − *Department of Civil and Environmental Engineering, The Pennsylvania State University, University Park, Pennsylvania 16802, United States;* orcid.org/0000-0001-7478-8070

Complete contact information is available at: https://pubs.acs.org/10.1021/acs.est.1c03010

Author Contributions

#X.Y. and Q.D. contributed equally to this work.

Notes

The authors declare no competing financial interest.

■ ACKNOWLEDGMENTS

This work was financially supported by the National Natural Science Foundation of China (nos. 51922051, 21876090, and 22036004), the fund for Distinguished Young Scholars of Tianjin (20JCJQJC00040), the fundamental research funds for the central universities (63213077 and 63213071), and the Ministry of Education of China (T2017002).

■ REFERENCES

(1) Ishii, S. I.; Suzuki, S.; Norden-Krichmar, T. M.; Tenney, A.; Chain, P. S. G.; Scholz, M. B.; Nealson, K. H.; Bretschger, O. A novel metatranscriptomic approach to identify gene expression dynamics during extracellular electron transfer. *Nat. Commun.* **2013**, *4*, 1601.

(2) Xiao, Y.; Zhang, E.; Zhang, J.; Dai, Y.; Yang, Z.; Christensen, H. E. M.; Ulstrup, J.; Zhao, F. Extracellular polymeric substances are transient media for microbial extracellular electron transfer. *Sci. Adv.* **2017**, *3*, No. e1700623.
(3) Reguera, G.; McCarthy, K. D.; Mehta, T.; Nicoll, J. S.; Tuominen, M. T.; Lovley, D. R. Extracellular electron transfer via microbial nanowires. *Nature* **2005**, *435*, 1098−1101.
(4) Wang, H.; Luo, H.; Fallgren, P. H.; Jin, S.; Ren, Z. J. Bioelectrochemical system platform for sustainable environmental remediation and energy generation. *Biotechnol. Adv.* **2015**, *33*, 317−334.
(5) Logan, B. E.; Rossi, R.; Ragab, A. A.; Saikaly, P. E. Electroactive microorganisms in bioelectrochemical systems. *Nat. Rev. Microbiol.* **2019**, *17*, 307−319.
(6) Lu, L.; Lobo, F. L.; Xing, D.; Ren, Z. J. Active harvesting enhances energy recovery and function of electroactive microbiomes in microbial fuel cells. *Appl. Energy* **2019**, *247*, 492−502.
(7) Mei, X.; Wang, H.; Hou, D.; Lobo, F. L.; Xing, D.; Ren, Z. J. Shipboard bilge water treatment by electrocoagulation powered by microbial fuel cells. *Front. Env. Sci. Eng.* **2019**, *13*, 53.
(8) Kumar, R.; Singh, L.; Zularisam, A. W. Exoelectrogens: recent advances in molecular drivers involved in extracellular electron transfer and strategies used to improve it for microbial fuel cell applications. *Renewable Sustainable Energy Rev.* **2016**, *56*, 1322−1336.
(9) Malvankar, N. S.; Tuominen, M. T.; Lovley, D. R. Lack of cytochrome involvement in long-range electron transport through conductive biofilms and nanowires of Geobacter sulfurreducens. *Energy Environ. Sci.* **2012**, *5*, 8651−8659.
(10) Reguera, G.; Kashefi, K. The electrifying physiology of Geobacter bacteria, 30 years on. In *Advances in Microbial Physiology*; Poole, R. K., Ed.; Academic Press, 2019; Vol. *74*, pp 1−96.
(11) Yan, X.; Lee, H.-S.; Li, N.; Wang, X. The micro-niche of exoelectrogens influences bioelectricity generation in bioelectrochemical systems. *Renewable Sustainable Energy Rev.* **2020**, *134*, 110184.
(12) Mahmoud, M.; Torres, C. I.; Rittmann, B. E. Changes in glucose fermentation pathways as a response to the free ammonia concentration in microbial electrolysis cells. *Environ. Sci. Technol.* **2017**, *51*, 13461−13470.
(13) Ren, L.; Zhang, X.; He, W.; Logan, B. E. High current densities enable exoelectrogens to outcompete aerobic heterotrophs for substrate. *Biotechnol. Bioeng.* **2014**, *111*, 2163−2169.
(14) Qu, Y.; Feng, Y.; Wang, X.; Logan, B. E. Use of a coculture to enable current production by Geobacter sulfurreducens. *Appl. Environ. Microbiol.* **2012**, *78*, 3484−3487.
(15) Huang, H.; Cheng, S.; Yang, J.; Li, C.; Sun, Y.; Cen, K. Effect of nitrate on electricity generation in single-chamber air cathode microbial fuel cells. *Chem. Eng. J.* **2018**, *337*, 661−670.
(16) Wan, Y.; Huang, Z.; Zhou, L.; Li, T.; Liao, C.; Yan, X.; Li, N.; Wang, X. Bioelectrochemical ammoniation coupled with microbial electrolysis for nitrogen recovery from nitrate in wastewater. *Environ. Sci. Technol.* **2020**, *54*, 3002−3011.
(17) Li, T.; Zhou, Q.; Zhou, L.; Yan, Y.; Liao, C.; Wan, L.; An, J.; Li, N.; Wang, X. Acetate limitation selects Geobacter from mixed inoculum and reduces polysaccharide in electroactive biofilm. *Water Res.* **2020**, *177*, 115776.
(18) Zhu, X.; Yates, M. D.; Hatzell, M. C.; Ananda Rao, H.; Saikaly, P. E.; Logan, B. E. Microbial community composition is unaffected by anode potential. *Environ. Sci. Technol.* **2014**, *48*, 1352−1358.
(19) Malvankar, N. S.; Lau, J.; Nevin, K. P.; Franks, A. E.; Tuominen, M. T.; Lovley, D. R. Electrical conductivity in a mixed-species biofilm. *Appl. Environ. Microbiol.* **2012**, *78*, 5967−5971.
(20) Tejedor-Sanz, S.; Fernández-Labrador, P.; Hart, S.; Torres, C. I.; Esteve-Núñez, A. Geobacter dominates the inner layers of a stratified biofilm on a fluidized anode during brewery wastewater treatment. *Front. Microbiol.* **2018**, *9*, 378.
(21) Cao, M.; Feng, Y.; Wang, N.; Li, Y.; Li, N.; Liu, J.; He, W. Electrochemical regulation on the metabolism of anode biofilms under persistent exogenous bacteria interference. *Electrochim. Acta* **2020**, *340*, 135922.
(22) Kondaveeti, S.; Lee, S.-H.; Park, H.-D.; Min, B. Specific enrichment of different Geobacter sp. in anode biofilm by varying interspatial distance of electrodes in air-cathode microbial fuel cell (MFC). *Electrochim. Acta* **2020**, *331*, 135388.
(23) Yamashita, T.; Ishida, M.; Asakawa, S.; Kanamori, H.; Sasaki, H.; Ogino, A.; Katayose, Y.; Hatta, T.; Yokoyama, H. Enhanced electrical power generation using flame-oxidized stainless steel anode in microbial fuel cells and the anodic community structure. *Biotechnol. Biofuels* **2016**, *9*, 62.
(24) Du, Q.; Mu, Q.; Cheng, T.; Li, N.; Wang, X. Real-time imaging revealed that exoelectrogens from wastewater are selected at the center of a gradient electric field. *Environ. Sci. Technol.* **2018**, *52*, 8939−8946.
(25) Prokhorova, A.; Sturm-Richter, K.; Doetsch, A.; Gescher, J. Resilience, dynamics, and interactions within a model multispecies exoelectrogenic-biofilm community. *Appl. Environ. Microbiol.* **2017**, *83*, No. e03033.
(26) Corbella, C.; Steidl, R. P.; Puigagut, J.; Reguera, G. Electrochemical characterization of Geobacter lovleyi identifies limitations of microbial fuel cell performance in constructed wetlands. *Int. Microbiol.* **2017**, *20*, 55−64.
(27) Bond, D. R.; Lovley, D. R. Electricity production by Geobacter sulfurreducens attached to electrodes. *Appl. Environ. Microbiol.* **2003**, *69*, 1548−1555.
(28) Lin, W. C.; Coppi, M. V.; Lovley, D. R. Geobacter sulfurreducens can grow with oxygen as a terminal electron acceptor. *Appl. Environ. Microbiol.* **2004**, *70*, 2525−2528.
(29) Sun, D.; Call, D.; Wang, A.; Cheng, S.; Logan, B. E. Geobacter sp SD-1 with enhanced electrochemical activity in high-salt concentration solutions. *Env. Microbiol. Rep.* **2014**, *6*, 723−729.
(30) Sun, D.; Wang, A.; Cheng, S.; Yates, M.; Logan, B. E. Geobacter anodireducens sp nov., an exoelectrogenic microbe in bioelectrochemical systems. *Int. J. Syst. and Evol. Microbiol.* **2014**, *64*, 3485−3491.
(31) Sun, D.; Call, D. F.; Kiely, P. D.; Wang, A.; Logan, B. E. Syntrophic interactions improve power production in formic acid fed MFCs operated with set anode potentials or fixed resistances. *Biotechnol. Bioeng.* **2012**, *109*, 405−414.
(32) Prodan, A.; Tremaroli, V.; Brolin, H.; Zwinderman, A. H.; Nieuwdorp, M.; Levin, E. Comparing bioinformatic pipelines for microbial 16S rRNA amplicon sequencing. *PLoS One* **2020**, *15*, No. e0227434.
(33) An, J.; Li, N.; Wan, L.; Zhou, L.; Du, Q.; Li, T.; Wang, X. Electric field induced salt precipitation into activated carbon air-cathode causes power decay in microbial fuel cells. *Water Res.* **2017**, *123*, 369−377.
(34) Zhou, L.; Yan, X.; Yan, Y.; Li, T.; An, J.; Liao, C.; Li, N.; Wang, X. Electrode potential regulates phenol degradation pathways in oxygen-diffused microbial electrochemical system. *Chem. Eng. J.* **2020**, *381*, 122663.
(35) Call, D. F.; Logan, B. E. A method for high throughput bioelectrochemical research based on small scale microbial electrolysis cells. *Biosens. Bioelectron.* **2011**, *26*, 4526−4531.
(36) Zhang, F.; Pant, D.; Logan, B. E. Long-term performance of activated carbon air cathodes with different diffusion layer porosities in microbial fuel cells. *Biosens. Bioelectron.* **2011**, *30*, 49−55.
(37) Caccavo, F., Jr.; Lonergan, D. J.; Lovley, D. R.; Davis, M.; Stolz, J. F.; McInerney, M. J. Geobacter sulfurreducens sp. nov., a hydrogen- and acetate-oxidizing dissimilatory metal-reducing microorganism. *Appl. Environ. Microbiol.* **1994**, *60*, 3752−3759.
(38) Coppi, M. V.; Leang, C.; Sandler, S. J.; Lovley, D. R. Development of a genetic system for Geobacter sulfurreducens. *Appl. Environ. Microbiol.* **2001**, *67*, 3180−3187.
(39) Sun, D.; Cheng, S.; Wang, A.; Li, F.; Logan, B. E.; Cen, K. Temporal-spatial changes in viabilities and electrochemical properties of anode biofilms. *Environ. Sci. Technol.* **2015**, *49*, 5227−5235.
(40) Böttcher, T.; Kolodkin-Gal, I.; Kolter, R.; Losick, R.; Clardy, J. Synthesis and activity of biomimetic biofilm disruptors. *J. Am. Chem. Soc.* **2013**, *135*, 2927−2930.

https://doi.org/10.1021/acs.est.1c03010
Environ. Sci. Technol. 2021, 55, 14928−14937

(41) Qu, L.; She, P.; Wang, Y.; Liu, F.; Zhang, D.; Chen, L.; Luo, Z.; Xu, H.; Qi, Y.; Wu, Y. Effects of norspermidine on Pseudomonas aeruginosa biofilm formation and eradication. *Microbiologyopen* **2016**, *5*, 402−412.
(42) Callahan, B. J.; McMurdie, P. J.; Rosen, M. J.; Han, A. W.; Johnson, A. J. A.; Holmes, S. P. DADA2: High-resolution sample inference from Illumina amplicon data. *Nat. Methods* **2016**, *13*, 581−583.
(43) Ward, T.; Larson, J.; Meulemans, J.; Hillmann, B.; Lynch, J.; Sidiropoulos, D.; Spear, J. R.; Caporaso, G.; Blekhman, R.; Knight, R. BugBase predicts organism-level microbiome phenotypes, **2017**. bioRxiv:10.1101/133462; p 133462.
(44) Liao, C.; Zhao, Q.; Wang, S.; Yan, X.; Li, T.; Zhou, L.; An, J.; Yan, Y.; Li, N.; Wang, X. Excessive extracellular polymeric substances induced by organic shocks accelerate electron transfer of oxygen reducing biocathode. *Sci. Total Environ.* **2021**, *774*, 145767.
(45) Dubois, M.; Gilles, K. A.; Hamilton, J. K.; Rebers, P. A.; Smith, F. Colorimetric method for determination of sugars and related substances. *Anal. Chem.* **1956**, *28*, 350−356.
(46) Sun, G.; Kang, K.; Qiu, L.; Guo, X.; Zhu, M. Electrochemical performance and microbial community analysis in air cathode microbial fuel cells fuelled with pyroligneous liquor. *Bioelectrochemistry* **2019**, *126*, 12−19.
(47) Paitier, A.; Godain, A.; Lyon, D.; Haddour, N.; Vogel, T. M.; Monier, J.-M. Microbial fuel cell anodic microbial population dynamics during MFC start-up. *Biosens. Bioelectron.* **2017**, *92*, 357−363.
(48) Wirsen, C. O.; Sievert, S. M.; Cavanaugh, C. M.; Molyneaux, S. J.; Ahmad, A.; Taylor, L. T.; DeLong, E. F.; Taylor, C. D. Characterization of an autotrophic sulfide-oxidizing marine Arcobacter sp that produces filamentous sulfur. *Appl. Environ. Microbiol.* **2002**, *68*, 316−325.
(49) Inoue, K.; Leang, C.; Franks, A. E.; Woodard, T. L.; Nevin, K. P.; Lovley, D. R. Specific localization of the c-type cytochrome OmcZ at the anode surface in current-producing biofilms of Geobacter sulfurreducens. *Env. Microbiol. Rep.* **2011**, *3*, 211−217.
(50) Wu, Y.; Zaiden, N.; Cao, B. The core- and pan-genomic analyses of the genus Comamonas: from environmental adaptation to potential virulence. *Front. Microbiol.* **2018**, *9*, 3096.
(51) Narayan, K. D.; Pandey, S. K.; Das, S. K. Characterization of Comamonas thiooxidans sp nov., and comparison of thiosulfate oxidation with Comamonas testosteroni and Comamonas composti. *Curr. Microbiol.* **2010**, *61*, 248−253.
(52) Marsili, E.; Sun, J.; Bond, D. R. Voltammetry and growth physiology of Geobacter sulfurreducens biofilms as a function of growth stage and imposed electrode potential. *Electroanal* **2010**, *22*, 865−874.
(53) Zhuang, Z.; Yang, G.; Mai, Q.; Guo, J.; Liu, X.; Zhuang, L. Physiological potential of extracellular polysaccharide in promoting Geobacter biofilm formation and extracellular electron transfer. *Sci. Total Environ.* **2020**, *741*, 140365.
(54) Dieltjens, L.; Appermans, K.; Lissens, M.; Lories, B.; Kim, W.; Van der Eycken, E. V.; Foster, K. R.; Steenackers, H. P. Inhibiting bacterial cooperation is an evolutionarily robust anti-biofilm strategy. *Nat. Commun.* **2020**, *11*, 107.
(55) Sapireddy, V.; Katuri, K. P.; Muhammad, A.; Saikaly, P. E. Competition of two highly specialized and efficient acetoclastic electroactive bacteria for acetate in biofilm anode of microbial electrolysis cell. *npj Biofilms Microbiomes* **2021**, *7*, 47.
(56) Wang, S.; An, J.; Wan, Y.; Du, Q.; Wang, X.; Cheng, X.; Li, N. Phosphorus competition in bioinduced vivianite recovery from wastewater. *Environ. Sci. Technol.* **2018**, *52*, 13863−13870.
(57) Unden, G. Transcriptional regulation and energetics of alternative respiratory pathways in facultatively anaerobic bacteria. *Biochim. Biophys. Acta, Bioenerg.* **1998**, *1365*, 220−224.
(58) Koike, I.; Hattori, A. Growth yield of a denitrifying bacterium, Pseudomonas denitrificans, under aerobic and denitrifying conditions. *J. Gen. Microbiol.* **1975**, *88*, 1−10.
(59) Esteve-Nunez, A.; Rothermich, M.; Sharma, M.; Lovley, D. Growth of Geobacter sulfurreducens under nutrient-limiting conditions in continuous culture. *Environ. Microbiol.* **2005**, *7*, 641−648.
(60) Mollaei, M.; Timmers, P. H. A.; Suarez-Diez, M.; Boeren, S.; Gelder, A. H.; Stams, A. J. M.; Plugge, C. M. Comparative proteomics of Geobacter sulfurreducens PCA(T) in response to acetate, formate and/or hydrogen as electron donor. *Environ. Microbiol.* **2021**, *23*, 299−315.
(61) Nealson, K. H.; Saffarini, D. Iron and manganese in anaerobic respiration: environmental significance, physiology, and regulation. *Annu. Rev. Microbiol.* **1994**, *48*, 311−343.
(62) Summers, Z. M.; Fogarty, H. E.; Leang, C.; Franks, A. E.; Malvankar, N. S.; Lovley, D. R. Direct exchange of electrons within aggregates of an evolved syntrophic coculture of anaerobic bacteria. *Science* **2010**, *330*, 1413−1415.
(63) Liu, X.; Zhuo, S.; Rensing, C.; Zhou, S. Syntrophic growth with direct interspecies electron transfer between pili-free Geobacter species. *Isme J* **2018**, *12*, 2142−2151.

https://doi.org/10.1021/acs.est.1c03010
Environ. Sci. Technol. 2021, 55, 14928−14937